The effect of oxygen content on the magnetic cluster in the paramagnetic region of $La_{0.67}Ca_{0.33}MnO_y$

2004 J. Phys.: Condens. Matter 16 7083

(http://iopscience.iop.org/0953-8984/16/39/039)

INSTITUTE OF PHYSICS PUBLISHING JOURNAL OF PHYSICS: CONDENSED MATTER

J. Phys.: Condens. Matter **16** (2004) 7083–7093 PII: S0953-8984(04)78221-1

The effect of oxygen content on the magnetic cluster in the paramagnetic region of $La_{0.67}Ca_{0.33}MnO_y$

Y Q Ma[1], W H Song[1], J Yang[1], B C Zhao[1], R L Zhang[1], Z G Sheng[1], W J Lu[1], G H Zheng[1], J M Dai[1], J J Du[1] and Y P Sun[1,2,3]

[1] Key Laboratory of Materials Physics, Institute of Solid State Physics, Chinese Academy of Sciences, Hefei 230031, People's Republic of China
[2] National Laboratory of Solid State Microstructures, Nanjing University, Nanjing 210008, People's Republic of China

E-mail: ypsun@issp.ac.cn

Received 22 March 2004
Published 17 September 2004
Online at stacks.iop.org/JPhysCM/16/7083
doi:10.1088/0953-8984/16/39/039

Abstract

We have measured the temperature dependence of internal friction $Q^{-1}(T)$, Young's modulus $E(T)$, and resistivity $\rho(T)$ *in situ* along with the measurements of magnetization $M(T)$ on optimally doped manganites $La_{0.67}Ca_{0.33}MnO_y$ with different oxygen contents. With the reduction of the oxygen content y, the Q^{-1} peak in the paramagnetic region, suggested to originate from the formation of the magnetic clusters (MC), shifts to a lower temperature and its magnitude decreases and finally disappears. The results of $M(T)$ and $\rho(T)$ indicates that both the effective magnetic moment μ_{eff} and the hopping distance of electrons decrease with the increase of oxygen vacancies, which may suppress the MC. In addition, the analysis of the results of $E(T)$ indicates that the cooperative effects of lattice distortions may favour the formation of MC.

1. Introduction

The discovery of 'colossal' magnetoresistance (CMR) in perovskite structure manganites $A_{1-x}A'_xMnO_3$ (here A is a rare earth such as La, Nd, Pr, Y and A′ is divalent element such as Ca, Sr, Ba, Pb) has stimulated extensive investigations of the structural, transport and magnetic properties of these materials [1]. The basic physics of manganites have primarily been described by the double-exchange (DE) model [2]. However, the DE model has some difficulties in explaining the magnitude of resistivity at high temperature and CMR quantitatively, and alternative mechanisms have been proposed. Several theoretical studies indicate that the formation of small polarons in the paramagnetic (PM) state due to strong electron–phonon coupling should be involved in explaining the basic physics of doped

[3] Author to whom any correspondence should be addressed.

manganites besides the DE interaction [3–5]. In addition to the small lattice polaron in PM state, De Teresa *et al* recently detected the presence of magnetic polarons (small ferromagnetic (FM) clusters whose size is determined to be about 12 Å in the PM region) below $1.8T_c$ using the small-angle neutron-scattering technique [6]. The results of the electron paramagnetic resonance also observed that the correlated moments per formula unit for $La_{0.67}Ca_{0.33}MnO_3$ air-annealed ($T_c \sim 270$ K) have an effective spin of $\sim$30 at $T = 280$ K [7].

Due to the strong correlation among spin, lattice and charge freedom degrees in manganites, the formation of the magnetic polaron has an influence on the lattice, electric transport and magnetic properties above T_c. An anomalous volume thermal expansion, which reflects the lattice distortion, is observed accompanying the presence of small MC above T_c in $La_{2/3}Ca_{1/3}MnO_3$, and the volume expansion is suggested to be associated with the gradual localization of the charge carriers below $\sim 1.8T_c$. Meanwhile, the appearance of MC in the PM region results in corresponding changes in the magnetization behaviour, i.e. a deviation of the inverse magnetic susceptibility $1/\chi$ from the Curie–Weiss law, $\chi = C/(T - \Theta)$, below $1.8T_c$ [6]. Besides the lattice and magnetization's response to the MC, the electrical transport is also involved. For $A_{0.7}B_{0.3}MnO_3$ (here A is La or Nd and B is Sr, Ca, etc), the resistivity best follows the variable-range hopping (VRH), and the electrons may be localized in FM wave packets [8, 9]. Additionally, the MC can be modified by the hole concentration x [10] and the substitution on B-site [11]. In addition, the variation of the oxygen content modifies the Mn^{3+}/Mn^{4+} ratio which plays an important role in the structural, electrical transport and magnetic properties of manganites [12, 13], and the formation of oxygen vacancy due to the reduction of oxygen content induces the lattice distortion. Therefore, changing the oxygen content can produce the important variables to test the MC in the PM region. However, literature seldom reports the effect of oxygen stoichiometry on the PM state in manganites. The nature of MC in the PM region needs to be investigated further.

The internal friction measuring technique is a nondestructive but very sensitive tool for studying defects and microscopic processes in solids including strongly electron-correlated materials, such as cuprate high-temperature superconductors and manganites [14, 15]. In addition, the Young's modulus is very sensitive to the microscopic strain. In this paper, *in situ* measurements of the internal friction $Q^{-1}(T)$, Young's modulus $E(T)$, and resistivity $\rho(T)$ along with the magnetic measurements are performed on the $La_{0.67}Ca_{0.33}MnO_y$ polycrystalline material allowing us to obtain simultaneously the relevant underlying mechanism about the MC above the PM–FM transition temperature T_c.

2. Experimental details

We synthesized polycrystalline samples $La_{0.67}Ca_{0.33}MnO_y$ by the standard solid state reaction with La_2O_3, $CaCO_3$ and MnO_2 powders with repeated grinding and refiring at 1000 and 1200 °C for 24 h for several times. After the final grinding, the powder was pressed into bars with the dimension of $69 \times 4.2 \times 2.5\,mm^3$ and sintered at 1400 °C for 48 h with an intermediate regrinding, and slowly cooled to room temperature. The powder x-ray diffraction measurement was performed using a Philips X'pert PRO x-ray diffractometer with Cu K_α radiation at room temperature and was refined using a standard Rietveld technique. The resistivity ρ was measured by the conventional four-probe technique. The magnetic measurements were performed on a Quantum Design superconducting quantum interference device (SQUID) MPMS system ($2 \leqslant T \leqslant 400$ K, $0 \leqslant H \leqslant 5$ T). The oxygen content of the samples was determined by a redox (oxidation–reduction) titration in which the powder samples taken in a quartz crucible were dissolved in (1 + 1) sulfuric acid containing an excess of sodium oxalate,

and the excess sodium oxalate was titrated with permanganate standard solution. $Q^{-1}(T)$ and $E(T)$ were measured by the free decay method of a resonant bar in the acoustic frequency range with magnitude of the order of kHz using warming mode in a helium gas environment at the rate of 0.7 K min^{-1} under zero applied magnetic field. The sample was excited electromagnetically in the fundamental modes. The internal friction Q^{-1} is defined as follows [14]:

$$Q^{-1} = \frac{1}{n} \ln\left(\frac{A_0}{A_n}\right), \tag{1}$$

where n is the number of the vibration cycles, while the amplitude attenuates from A_0 to A_n. The Young's modulus E is given by

$$E = \frac{4\pi^2 sdl^4}{m^4 I} f^2, \tag{2}$$

where f is the resonant frequency, s the cross-sectional area, d the density, l the length and I the moment of inertia of the sample. In addition, $m = 4.730$ for the vibrating mode in the fundamental mode, in which the sample is suspended at two points whose span is $0.224l$ from the two free ends of the sample. Based on equation (2), E is proportional to the square of the resonant frequency, i.e. $E \propto f^2$. Therefore we substitute f^2 for the Young's modulus E. For the sake of convenience, the relative modulus is defined as $\Delta E = [f^2(T) - f^2_{\min}]/[f^2_{\max} - f^2_{\min}]$. Here, $f_{\min}$ and $f_{\max}$ are the minimum and maximum resonant frequencies in the whole measuring temperature range, respectively.

To change the oxygen content, we annealed the sample at temperatures 700, 800 and 850 °C in a N_2 atmosphere under 2 MPa pressure for 4 h with graphite powder near the sample [16]. The samples as-prepared, annealed in N_2 at temperatures 700, 800 and 850 °C are referred to as S_0, S_1, S_2 and S_3, respectively, in the discussion below.

3. Results and discussion

The oxygen content y of the sample is determined to be 3.02, 2.95, 2.88 and 2.85 corresponding to samples S_0, S_1, S_2 and S_3, respectively. Figure 1 presents the x-ray-diffraction patterns of samples at room temperature. The x-ray-diffraction data is refined by using a standard Rietveld technique and all diffraction peaks for S_0–S_3 samples can be indexed by an orthorhombic lattice with space group Pbnm, indicating that no structure (symmetry) variations occur on changing the oxygen. However, all diffraction peaks shift to below the angle 2θ on reducing y. The unit cell volumes of S_0–S_3 samples deduced from the x-ray-diffraction data are 231.11, 231.16, 231.34 and 231.99 $Å^3$. The increase of the unit cell volume with the reduction of the oxygen content originates from the increase of the average manganese ionic size due to the decrease of the average manganese oxidation state because of increasing oxygen deficiency.

Based on our previous study [17], the sample S_0 with $y = 3.02$ exhibits a PM–FM transition at 251 K. The inverse magnetic susceptibility $1/\chi$ deviates from the Curie–Weiss law above T_c up to 330 K. A deviation of $1/\chi$ from the Curie–Weiss law is very common in the conventional non-manganite materials, and it reveals the existence of the ferromagnetic fluctuations above T_c. Figure 2 shows the temperature dependence of internal friction $Q^{-1}(T)$ and Young's modulus $E(T)$ of the S_0 sample. $Q^{-1}(T)$ in the FM region is qualitatively similar to our previous study [15]. Besides this, $Q^{-1}(T)$ of S_0 exhibits a strong Q^{-1} peak at the temperature above T_c, 330 K ($\sim 1.3T_c$), which approaches the onset temperature of $1/\chi$ deviating from the Curie–Weiss law. So it is suggested that the origin of the Q^{-1} peak at 330 K may be closely

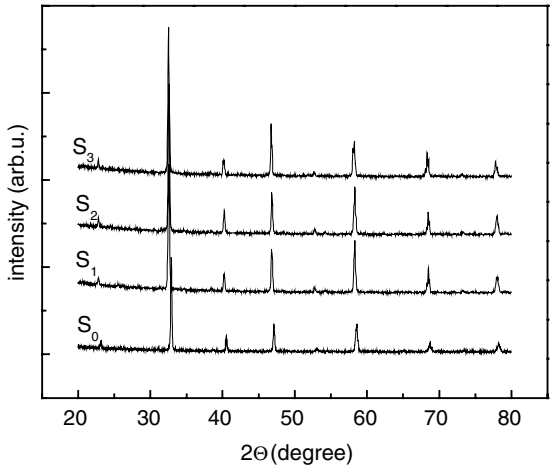

Figure 1. X-ray-diffraction patterns of the S_0–S_3 samples.

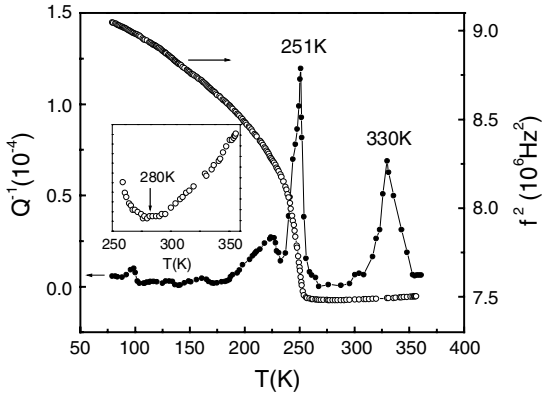

Figure 2. Temperature dependence of internal friction $Q^{-1}(T)$ and Young's modulus $E(T)$ (denoted by the square of the resonant frequency f^2) for S_0. The inset shows the magnified plot of E around the minimum at 280 K.

related to the formation of MC in the PM region. In order to support the above suggestion, we analyse the $\rho(T)$ data in the PM region. In the perovskite manganite which is a spin–charge–lattice strongly correlated system, the local variation of magnetic structure modifies the transport mechanism. Figure 3 shows the temperature dependence of resistivity $\rho(T)$ (open circles) and it presents a metal–insulator transition (MIT) at 259 K. By fitting, we find that $\rho(T)$ data in the whole temperature range above MIT cannot be described by a single conducting mechanism. Specifically, $\rho(T)$ data follows Mott's variable-range-hopping (VRH) law, $\rho(T) = \rho_0 \exp(T_0/T)^{1/4}$ in the temperature range of $259 < T < 320$ K and the adiabatic small polaronic conduction (SPC) law, $\rho(T) = \rho_0 T \exp(E_a/k_B T)$ in the temperature region of $350 < T < 550$ K, respectively. The fitting curves are also plotted in figure 3 as shown in dashed line L1 (denoting SPC law) and solid line L2 (denoting VRH law). The variation of the conduction mechanism is attributed to the formation of the MC in the PM region [8, 9].

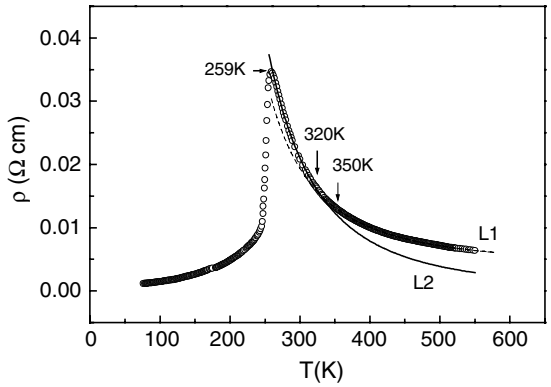

Figure 3. The experimental (○) and fitting (— and - - - -) curves of the resistivity of S_0. Lines L1 and L2 denote the fitting curve of $\rho(T)$ in terms of the small polaronic conduction law and the Mott's three-dimensional variable-range-hopping conduction law, respectively.

The existence of MC in the PM region has been evidenced in many previous studies on the variants of the Ruddlesden–Popper series $A_{n+1}B_nO_{3n+1}$ at $n = \infty$ [6, 7] and $n = 2$ [18]. For $SrO(La_{1-x}Sr_xMnO_3)_2$ ($x = 0.3$) [18] which has an ordering temperature of 72 K. However, even at $T = 120$ K, a clear hysteretic effect was observed in the low-field susceptibility, which is an indication of the ferromagnetism, and the TEM picture shows that intergrowths are stacking faults due to missing or extra layers of SrO between the MnO_6 octahedral planes. Such defects represent local inclusions of $n > 2$ variants of the Ruddlesden–Popper series which have a higher ordering temperature than the $n = 2$ host material and, therefore, cause a small soft-ferromagnetic background in the paramagnetic phase. However, there is a bit of difference between the $SrO(La_{1-x}Sr_xMnO_3)_2$ ($x = 0.3$) and $La_{1-x}Ca_xMnO_3$ systems. Cheong *et al* studied the phase behaviour in $La_{1-x}Ca_xMnO_3$ and the authors found a maximum for $x = 3/8$ in the FM T_c at 272 K [1]. T_c of any new phase of the local inhomogeneity of the sample chemistry is lower than 272 K. This is also described in a previous study [19], i.e. bulk $La_{1-x}Ca_xMnO_3$ material exhibits a doping-dependent maximum T_c value at the nominal composition of $x = 1/3$, and any chemical inhomogeneity should shift the T_c-distribution to a lower temperature. In addition, non-stoichiometric oxygen may cause the defects of La and Mn sites [20], which also decreases T_c. So it is reasonable to suggest that the Q^{-1} peak at 330 K for the sample S_0 may not result from the chemical inhomogeneity, and there may be some other mechanism. We suggest that the appearance of MC in the sample S_0 is closely related to the local lattice distortion disorder of the $Mn^{3+}O_6$ octahedron which belongs to the phase separation induced by disorder as argued by Moreo *et al* [10]. De Teresa *et al* [6] suggested that a localized electron causes the local lattice distortion, macroscopically, the volume expansion, and, if an electron which becomes localized polarizes the spins of the neighbouring ions due to FM exchange interaction, a magnetic polaron would be formed. To further understand the nature of MC in the PM region, the effect of the oxygen on MC in the PM matrix is investigated, which is the main purpose of this paper.

Figure 4 shows the temperature dependence of magnetization $M(T)$ of the samples S_1, S_2 and S_3 with $y = 2.95$, 2.88 and 2.85, respectively, measured in a field of 0.01 T. Both zero-field-cooling (ZFC) and field-cooling (FC) data were recorded. The PM–FM transition temperature T_c, defined as the inflection point on the $M(T)$ curve, are 253, 164, and 73 K. PM–FM transition becomes broader on decreasing the oxygen content y, which may be attributed to a distribution of T_c values [19].

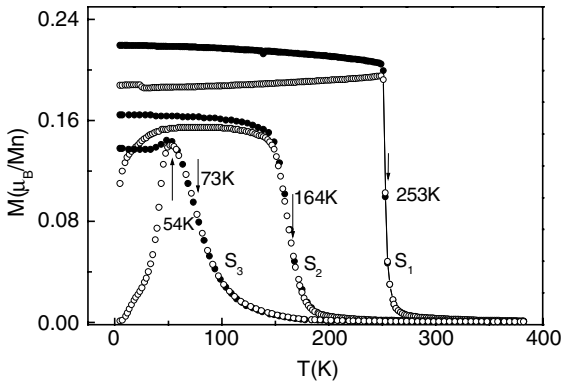

Figure 4. Magnetization (M) as a function of temperature for samples S_1, S_2 and S_3. Both zero-field-cooling (ZFC) (○) and field-cooling (FC) (●) data are recorded in an applied field of 0.01 T.

The temperature dependence of resistivity $\rho(T)$ and relative modulus $\Delta E(T)$ is shown in figures 5(a)–(c) for the samples S_1, S_2 and S_3 respectively. As shown in figure 5(a), $\rho(T)$ for S_1 shows a distinct MIT at $T_p \sim 257$ K. In the process of MIT, $\Delta E(T)$ exhibits rapid softening with increasing temperature implying that there exists a close correlation between charge and lattice. The temperature dependence of $\rho(T)$ and $\Delta E(T)$ for S_2 are shown in figure 5(b). T_p of the sample S_2 shifts to 148 K, and the resistivity $\rho(T)$ is of about three orders of magnitude larger than that of S_1. $\Delta E(T)$ shows slow softening when MIT occurs. For the S_3 sample, the magnitude of $\rho(T)$ is of about seven orders of magnitude larger than that of the sample S_1, and MIT disappears, as shown in figure 5(c), which indicates that the large amount of oxygen vacancies makes the FM percolative conducting path break down resulting in the disappearance of MIT. In the PM insulating region, $\rho(T)$ of S_1, S_2 and S_3 exhibits a monotonic decrease with increasing temperature and does not show any anomalous change with the variation of the oxygen content and temperature.

The temperature dependence of $Q^{-1}(T)$ and $E(T)$ measured *in situ* with $\rho(T)$ for S_1, S_2 and S_3 is shown in figures 6(a)–(c), which exhibit the more microscopic behaviour in the PM region. Figures 6(a) and (b) show that there appears a Q^{-1} peak at 253 K for the sample S_1 and at 164 K for S_2, and the height of Q^{-1} peak decreases with y reduction. Combined with the results of $M(T)$ as shown in figure 4, both the 253 and 164 K Q^{-1} peaks can be attributed to a PM–FM transition. For S_3 with $y = 2.85$, $T_c \sim 73$ K is beyond the temperature range of Q^{-1} measurement. For the samples S_2 and S_3, the Q^{-1} magnitude has a steep rise below around 110 K compared with that of the samples S_0 and S_1. As is well known, the Young's modulus E is closely related to cohesive force among atoms and is proportional to the inverse of the static strain if the external force is kept constant. Therefore the behaviour of E actually provides information about the behaviour of lattice variations. It can be seen from the inset of figure 6(c) that $E(T)$ values for S_2 and S_3 are much lower than those of S_0 and S_1 in the whole temperature range, which indicates that the reduction of y results in the lattice distortion. Combining the results of $M(T)$ with the Young's modulus $E(T)$, it is suggested that a steep rise in the Q^{-1} magnitude below around 110 K for the samples S_2 and S_3 may result from the variation of magnetic coupling and lattice distortion with an increase in the oxygen vacancies.

Now we would like to discuss the oxygen stoichiometric effect on the properties of the paramagnetic state in $La_{0.67}Ca_{0.33}MnO_y$. For the S_1 sample with $y = 2.95$, there appears a distinct Q^{-1} peak at 295 K, $\sim 1.2T_c$, which is higher than the highest T_c, 272 K,

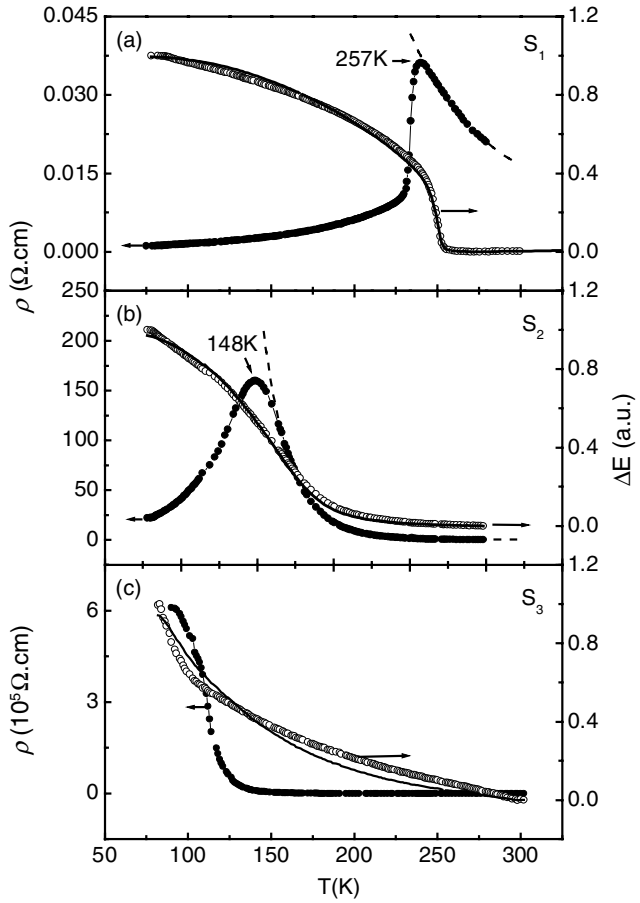

Figure 5. The temperature dependence of resistivity $\rho(T)$ and relative modulus $\Delta E(T)$ for the samples (a) S_1, (b) S_2 and (c) S_3. The dark solid lines are fitting curves of $\Delta E(T)$ according to $\Delta E = \tanh[\Delta E/(T/T_D)]$ and the dashed lines are fitting curves of resistivity $\rho(T)$.

mentioned above indicating that this Q^{-1} peak does not result from the new phase of chemical inhomogeneity which has a lower T_c value. On reducing the oxygen content y to 2.88, the Q^{-1} peak above T_c decreases to 188 K, $\sim 1.1T_c$, which is argued to have the same origin as that of S_0 and S_1, and the height of Q^{-1} peak also decreases on reducing y. When the oxygen content is reduced to $y = 2.85$, the Q^{-1} peak above T_c disappears for the sample S_3 as shown in figure 6(c). Compared with the Q^{-1} peak at T_c, whose height seems to correlate with the magnitude of M, it is easily deduced that the height of Q^{-1} peak above T_c may also be related to the magnetic properties.

Figure 7 shows the temperature dependence of the inverse of the magnetic susceptibility $1/\chi_M$ for S_1, S_2 and S_3, respectively. Solid lines denote the fitting curves according to the Curie–Weiss equation, $\chi_M = C/(T - \Theta)$, where C is the Curie constant, and Θ is the PM Curie temperature. Some of the fitting parameters deduced from the Curie–Weiss equation are as follows. The values of the Curie constant C are 7.45, 4.81 and 4.53 $cm^3\ mol^{-1}\ K$, corresponding to the PM Curie temperature Θ of 255, 195 and 142 K, respectively, for samples S_1, S_2 and S_3, which are higher than the corresponding T_c. Furthermore, the effective magnetic moments μ_{eff}

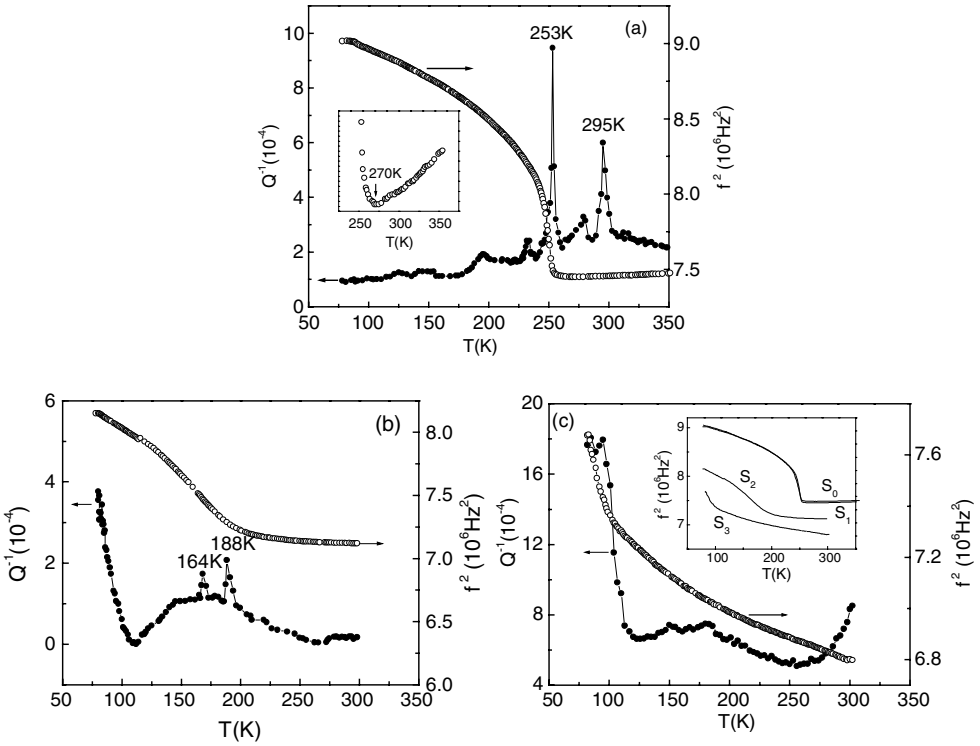

Figure 6. The temperature dependence of internal friction $Q^{-1}(T)$ and Young's modulus $E(T)$ (denoted by the square of the resonant frequency f^2) for (a) S_1, (b) S_2 and (c) S_3. The inset in (a) is a magnified plot of E around the minimum at 270 K. The inset in (c) shows moduli of the variables for all samples S_0, S_1, S_2 and S_3 for purposes of easy comparison.

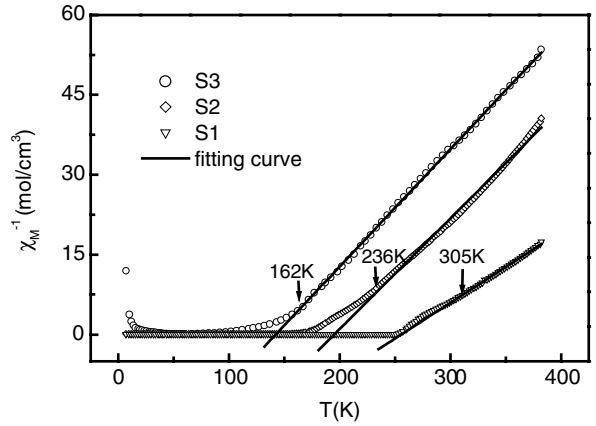

Figure 7. The temperature dependence of the inverse of the magnetic susceptibility $1/\chi_M$ for S_1, S_2 and S_3. The dark solid lines are the fitting curves according to the Curie–Weiss equation.

are deduced as 3.86, 3.10 and 3.01μ_B, for S_1, S_2 and S_3, respectively. The reduction of oxygen content increases the Mn^{3+}/Mn^{4+} ratio and drives the system to deviate from the optimum doping level $x = 0.33$ when the strongest DE FM coupling occurs. In addition, the reduced oxygen content also produces disordered oxygen vacancies and lattice distortion, and, as a result, the hopping magnitude of e_g electrons decreases which results in the weakening of DE interaction. These effects may be the possible reason for the reduction of μ_{eff} and the decrease of the height of the Q^{-1} peak above T_c.

In order to get further insight into MC in the PM region, we analyse $\rho(T)$ data of S_1, S_2 and S_3 based on the above description about the transport behaviour of S_0 in the insulating state. It is supposed that the resistivity best follows the variable-range-hopping (VRH), $\rho \propto \exp(T_0/T)^{1/4}$, in the temperature range where MC exists [8]. The resistivity of S_0, S_1 and S_2 can also be fitted by the VRH model in the PM insulating region above T_c. T_0 obtained from the fitting results is 1.17×10^7, 1.40×10^7 and 2.82×10^7 for S_0, S_1 and S_2, respectively. For the sample S_3, no MIT is observed and the resistivity does not satisfactorily follow any conducting mechanism that is usually used to describe the semiconductive-like transport behaviour [1]. If a random potential of magnetic origin is taken into account, which is responsible for the carrier localization above T_c, κT_0 is given by $\kappa T_0 = 171\alpha^3 U_m \nu$, where $1/\alpha$ is the localization length, $U_m = 3J_H/2$ the splitting between spin-up and spin-down e_g bands and ν is the lattice volume per manganese ion, $5.7 \times 10^{-29}\,m^3$ [8]. Taking $U_m = 2$ eV [21], the corresponding localization lengths for S_0, S_1 and S_2 are 0.27, 0.25 and 0.10 nm, respectively, which are in good agreement with the values in [8]. The average hopping distance of e_g electrons is given as $R = \{9/[8\pi\alpha N(E)\kappa T]\}^{1/4}$, approximately, $N(E) \approx 4 \times 10^{28}\,m^{-3}\,eV^{-1}$. Therefore, at room temperature, the values of the average hopping distance are 0.55, 0.54 and 0.42 nm, respectively [8]. That is to say, the average hopping distance of e_g electrons has a sudden decrease for y reducing from 3.02, 2.95 to 2.88. Based on the discussion of the magnetization and resistivity in the PM insulating region, both μ_{eff} and the average hopping distance of e_g electrons decrease with the reduction of the oxygen content. These variations do not favour DE interaction which may contribute to the suppressed and missed Q^{-1} peak above T_c.

According to [6], the formation of MC is associated with the lattice expansion, so the lattice variation induced by changing the oxygen content cannot be neglected. $E(T)$ of S_0 and S_1 shows a minimum around 280 and 270 K, respectively, as shown in the magnified plot in the insets of figures 2 and 6(a), reflecting the lattice expansion. In general, $E(T)$ is supposed to decrease monotonically with increasing temperature in the absence of additional effects. The anomalous minimum of E may be associated with the formation of MC, which is evidenced in the result obtained by De Teresa *et al* [6], i.e., the lattice expansion and MC are simultaneously present in the temperature range of T_c–$2T_c$ for the sample $La_{2/3}Ca_{1/3}MnO_3$. Unexpectedly, though there also exists a Q^{-1} peak at 188 K ($\sim 1.1T_c$), which may be attributed to the formation of MC, E of S_2 decreases monotonically with temperature above T_c increasing. We suggest that one possible way to interpret this result is to assume that the lattice expansion is not an indispensable condition and there may exist another underlying mechanism that is favourable to the presence of the MC.

For the sample S_1, the temperature dependence of the relative Young's modulus $\Delta E(T)$ in figure 5(a) is reminiscent of a characteristic behaviour of the lattice distortion caused by a cooperative Jahn–Teller (JT) effect [22]. For the $TmVO_4$ system, the cooperative JT distortion can be described by the expression derived from a mean-field approximation [23]:

$$e(T)/e^0 = \tanh[(e(T)/e^0)/(T/T_D)], \tag{3}$$

where e^0 is the static strain at the absolute zero temperature. We try to fit the $\Delta E(T)$ of S_1 using the equation:

$$\Delta E = \tanh[\Delta E/(T/T_D)]. \tag{4}$$

The fitting data match the experimental results well, which indicates that the lattice distortion in the sample S_1 is satisfied with the cooperative JT distortion. For the sample S_2, it has the higher concentration of Mn^{3+} ions compared with that of S_1 which results in the stronger JT effect, and $\Delta E(T)$ of S_2 can be better fitted by equation (4), compared with the fitting results of S_1. As mentioned above, no anomalous lattice expansion appears in the PM region of S_2, and hence we suppose that the cooperative JT distortion may favour the formation of MC. The cooperative JT distortion can be well understood in terms of the description of Burgy *et al* [24]: once a distortion is created, it propagates following a power-law decay $1/\gamma^{\alpha}$ governed by standard elasticity mechanism. This propagation emerges from the cooperative nature of the distortions, since the adjacent MnO_6 shares an oxygen. By means of the simulation using the RFIM (random field Ising model)-like toy models, Burgy *et al* suggested that clusters are larger in size with a consideration of the correlated distortion ($\alpha = 3$) than those obtained with uncorrelated distortion ($\alpha = \infty$) which indicates that the cooperative effects of lattice distortion favours the formation of clusters. On reducing the oxygen content y to 2.85, $La_{0.67}Ca_{0.33}MnO_{2.85}$ has the highest ratio of Mn^{3+}/Mn^{4+}. The higher concentration of Mn^{3+} JT ions should be beneficial to the formation of the cooperative JT distortion [25]. However, it is not the case for S_3. The experimental data $\Delta E(T)$ cannot be fitted by equation (4). This is easily understood considering that a large number of oxygen vacancies destroy the Mn–O–Mn network and make it difficult to form the long-range and uniform strain. That is to say, because the oxygen which links the adjacent MnO_6 octahedra is absent, an MnO_6 octahedral distortion fails to propagate following a power-law decay $1/\gamma^{\alpha}$ and the cooperation among the distortions is difficult to form which results in the much smaller clusters. This may be the main reason for the disappearance of the Q^{-1} peak of S_3 above T_c.

4. Conclusion

In situ measurements of $Q^{-1}(T)$, $E(T)$ and $\rho(T)$ along with measurements of the magnetic properties have been performed on the manganites $La_{0.67}Ca_{0.33}MnO_y$ with different oxygen content. On decreasing the oxygen content y, both the μ_{eff} and the average hopping distance of e_g electrons decrease which may contribute to the suppressed and missed Q^{-1} peak above T_c. In addition, it is proposed that the cooperative effects of lattice distortions may favour the formation of FM clusters in the PM region. The observed effect of the oxygen content on MC above T_c provides evidence for the close correlation among lattice, charge and spin freedom degrees in manganites.

Acknowledgments

This work was supported by the National Key Research under Contract No. 001CB610604, the National Nature Science Foundation of China under Contract Nos. 10174085 and 10074066, the Anhui Province NSF Grant No. 03046201 and the Fundamental Bureau Chinese Academy of Sciences.

References

[1] Ramirez A 1997 *J. Phys.: Condens. Matter* **9** 8171
Coey J M D, Viret M and Von Molnar S 1999 *Adv. Phys.* **48** 167
Tokura Y 2000 *Colossal Magnetoresistive Oxides* (New York: Gordon and Breach)
Salamon M B and Jaime M 2001 *Rev. Mod. Phys.* **73** 583
[2] Zener C 1951 *Phys. Rev.* **82** 403
Anderson P W and Hasegawa H 1955 *Phys. Rev.* **100** 675
[3] Millis A J, Littlewood P B and Shraiman B I 1995 *Phys. Rev. Lett.* **74** 5144
[4] Röder H, Zang J and Bishop A R 1996 *Phys. Rev. Lett.* **76** 1356
[5] Millis A J, Shraiman B I and Mueller R 1996 *Phys. Rev. Lett.* **77** 175
[6] De Teresa J M, Ibarra M R, Algarabel P A, Ritter C, Marquina C, Blasco J, Garcia J, del Moral A and Arnold Z 1997 *Nature* **386** 56
[7] Oseroff S B, Torikachvili M, Singley J, Ali S, Cheong S-W and Schultz S 1996 *Phys. Rev.* B **53** 6521
[8] Viret M, Ranno L and Coey F M D 1997 *Phys. Rev.* B **55** 8067
[9] Anil Kumar P S, Joy P A and Date S K 1998 *J. Phys.: Condens. Matter* **10** L269
[10] Moreo A, Yunoki S and Dagotto E 1999 *Science* **283** 2034
[11] Souza Filho A G *et al* 2003 *Phys. Rev.* B **67** 052405
[12] Ju H L, Gopalakrishnan J, Peng J L, Li Q, Xiong G C, Venkatesan T and Greene R L 1995 *Phys. Rev.* B **51** 6143
[13] Bukowski Z, Dabrowski B, Mais T, Klamut P W, Kolesnik S and Chmaissem O 2000 *J. Appl. Phys.* **87** 5031
[14] Du J J, Sun Y P, Jiang J Y, Zeng F C and Yin H Q 1990 *Phys. Rev.* B **41** 6679
[15] Ma Y Q, Song W H, Zhang R L, Dai J M, Yang J, Bi C Z, Ge Y J, Qiu X G, Du J J and Sun Y P 2004 *Phys. Rev.* B **69** 134404
[16] Zhao Y G *et al* 2002 *Phys. Rev.* B **65** 144406
[17] Ma Y Q, Song W H, Zhao B C, Dai J M, Zhang R L, Yang J, Sheng Z G, Lu W J, Du J J and Sun Y P 2004 *Phys. Rev.* B submitted
[18] Berger A, Mitchell J F, Miller D J and Bader S D 2001 *J. Appl. Phys.* **89** 6851
[19] Campillo G, Berger A, Osorio J, Pearson J E, Bader S D, Baca E and Prieto P 2001 *J. Magn. Magn. Mater.* **237** 61
Jin S, Tiefel T H, McCormack M, Fastnacht R A, Ramesh R and Chen L C 1994 *Science* **264** 413
[20] Roosmalen J A M van *et al* 1994 *J. Solid State Chem.* **110** 109
[21] Okimoto Y, Katsufuji T, Ishikawa T, Urushibara A, Arima T and Tokura Y 1995 *Phys. Rev. Lett.* **75** 109
[22] Feng D (ed) 1990 *Metallic Physics, vol. 2: Phase Transition* (Beijing: Scientific Publishing House of China) p 470
[23] Segmueller A, Melcher R L and Kinder H 1974 *Solid State Commun.* **15** 101
[24] Burgy J, Moreo A and Dagotto E 2004 *Phys. Rev. Lett.* **92** 097202
[25] Millis A J 1996 *Phys. Rev.* B **53** 8434